高エネルギー宇宙物理研究会 2020 (2020.12.14, 17)

3次元流体計算に基づく超新星1987Aの超新星爆発から超新星残骸までの進化

Masaomi Ono [1)], S. Orlando [2)], M. Miceli [3)], S. Nagataki [1)], Gilles Ferrand [1)], K. Takahashi [4)], H. Umeda [5)], T. Yoshida [5)], T. Nozawa [6)], O. Petruk [7)], F. Bocchino [2)], G. Peres [2)]

1) RIKEN, Japan, 2) INAF — Osservatorio Astronomico di Palermo, Italy, 3) Universita` di Palermo, Italy, 4) AEI, Germany, 5) University of Tokyo, Japan, 6) NAOJ, 7) Inst. Appl. Probl. in Mech. and Math., Ukraine

Abstract

More than 30 years have passed from the discovery of **SN 1987A**. However, the details of the explosion and the formation scenario of the progenitor (Sk – 69° 202) have not been elucidated. Early observations, e.g., [Fe II] line profiles (Haas et al. 1990) have insisted the existence of ***high velocity ^{56}Ni*** (> 4000 km/s) and ***matter mixing during the SN explosion***. After the explosion, the lights from the SN have illuminated the triple ring-like structure and the equatorial ring has been brightened in X-ray for more than a decade. SN 1987A gives us a ***unique opportunity to understand the transition from SN to supernova remnant (SNR)***. However, so far there is no 3D numerical model from SN to SNR consistent with such observations. Therefore, ***we perform 3D simulation from SN to SNR for SN 1987A for the first time in order to explain observed [Fe II] lines and X-ray emission*** **[4,5]**. Additionally, motivated by recent observation of 3D distribution of rotational transition lines from CO and SiO molecules (Abellán et al. 2017; Cigan et al. 2020) by ALMA, ***we perform molecule formation calculation based on the 3D SN simulation*** **[6]**.

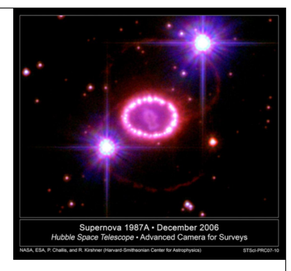

Initial Conditions and Method

Progenitor models for SN 1987A: Two progenitor models based on a single star evolution and a ***binary merger*** evolution.
1) **n16.3**: 16.3 $M_\odot$ single star BSG model (Shigeyama & Nomoto 1990)
2) **b18.3**: 18.3 $M_\odot$ BSG model based on a ***slow-merger scenario*** **[1]**.

3D simulation of SN explosion: 3D hydrodynamical simulation based on **[2]**. The hydrodynamic code: **FLASH** (Fryxell 2000) with a ***nuclear reaction network (19 nuclei)***. Initiation of explosions: injecting thermal and kinetic energy around the Fe/Si composition interface of the prog. star initially. Non-spherically distributed Initial radial velocity: an elliptical form (see **Fig. 1**). Basic model parameters: Injected energy (E_{in}), ratio of Initial radial velocity at the polar to equatorial region ($\beta = v_{pol}/v_{eq}$), asymmetry against the equatorial plane ($\alpha = v_{north}/v_{south}$).

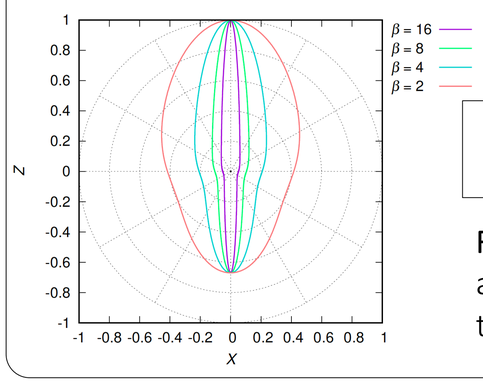

$$v_r \propto r \left(\beta^{-1}\cos^2\theta + \beta \sin^2\theta\right)^{-1/2}$$

Range of parameters investigated:
E_{in}: (1.5 – 3.0) x 10^{51} erg, β: 1.0 – 16.0, α: 1.0 – 2.0

Fig. 1 Distribution of initial radial velocity. Here, asymmetry against the equatorial plane is also taken into account.

3D MHD simulation of the SNR evolution: 3D MHD simulation based on **[3]**. The MHD code: **PLUTO** (Mignone et al. 2007). ***X-ray emission*** is estimated as a post-processing **[3]**. The equatorial ring is set at the start of the MHD simulation. As the initial condition, the 3D SN simulation results are used. During mapping of 3D SN simulation results into a new 3D grid for the 3D MHD simulation, the distributions are rotated to be consistent with the observed [Fe II] line profiles.

Results

Distributions of line of sight velocity of ^{56}Ni: The distribution of line of sight (LoS) velocity of ^{56}Ni corresponding to [Fe II] line profiles are compared with observations. From the comparison, the best explosion parameters and progenitor model are derived (See **Fig. 2**) **[4]**.

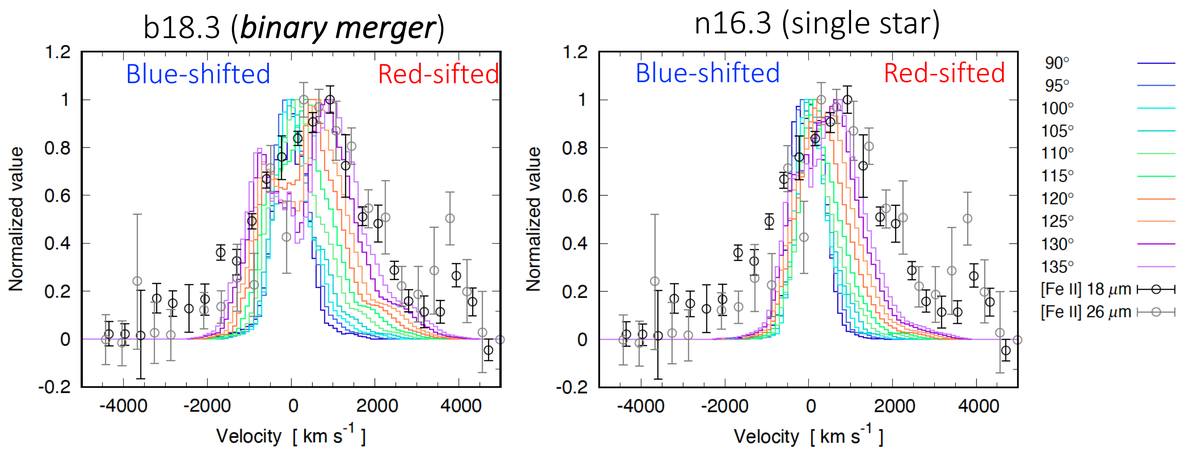

Fig. 2 Distribution of LoS velocity of ^{56}Ni. Dots with error bars: observed [Fe II] line profiles (18 μm and 26 μm: Haas et al. 1990). Solid lines are results from 3D SN simulation. Left (right) panel: b18.3 (n16.3).

The best parameter set: (E_{in}, α, β, progenitor model) = (2.5 x 10^{51} erg, 1.5, 16.0, b18.3)

Distributions of elements: Distributions of elements at just before the shock breakout (**Fig. 3**). Even if the explosion parameters are same, the morphology of inner SN ejecta depends on the progenitor model **[4]**.

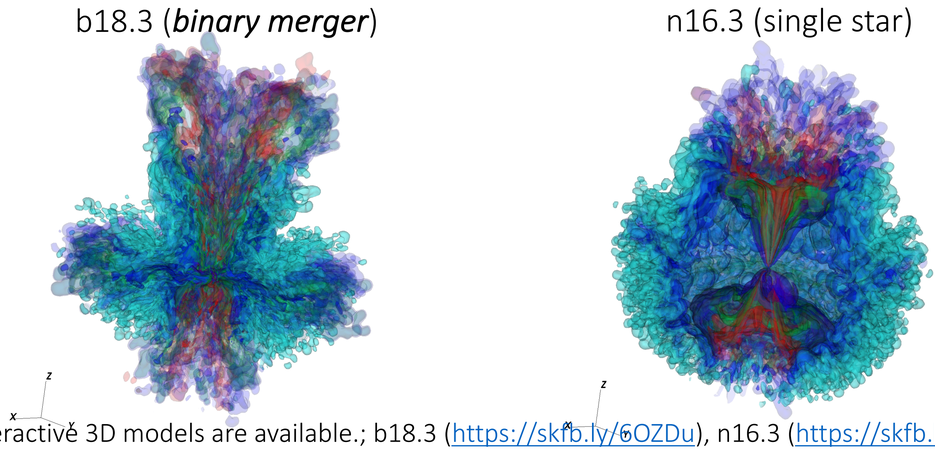

Interactive 3D models are available.; b18.3 (https://skfb.ly/6OZDu), n16.3 (https://skfb.ly/6OZDv).

Fig. 3 Distribution of elements. Left (right) panel: b18.3 (n16.3). For each element, two isosurfaces of 10% and 70% of the maximum mass fraction are shown. Red, green, blue, cyan are denote ^{56}Ni, ^{28}Si, ^{16}O, and ^{4}He, respectively.

X-ray light curves an images: Estimated X-ray light curves and images (**Fig. 4**). Both models well explain observed light curves within uncertainties of the ambient medium (ring, HII region, and wind components) **[5]**.

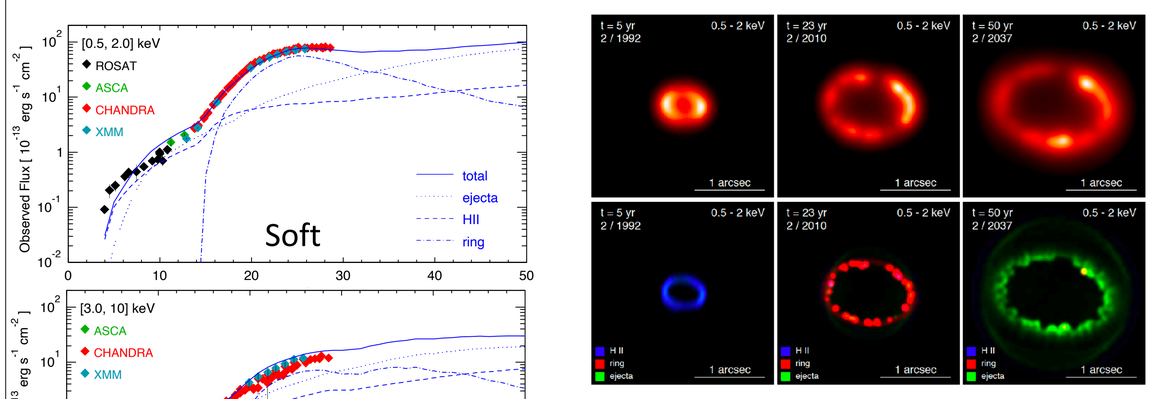

b18.3 (***binary merger***)

Fig. 4 Synthesized X-ray light curves, [0.5, 2.0] keV (left top) and [3.0,10] keV (left bottom) and X-ray images (right panels) for b18.3 at different epochs. Right bottom panels show contribution from different components (HII region (blue), ring (red), and ejecta (green)).

Molecule formation calculation: Based on 3D SN simulation results, molecule formation in the supernova ejecta is calculated **[6]** (**Fig. 5**) with small molecule formation network (including CO, SiO, SiC, … : 8 atoms and 10 molecules). For simplicity, power law profiles ($\rho(t) \propto t^{-3}$, $T(t) \propto t^{-0.75}$) are assumed as the density and temperature evolutions after about 1 day. A qualitative feature (SiO is concentrated at the center and CO surrounds SiO molecule) is similar to the observed one (Abellán et al. 2017).

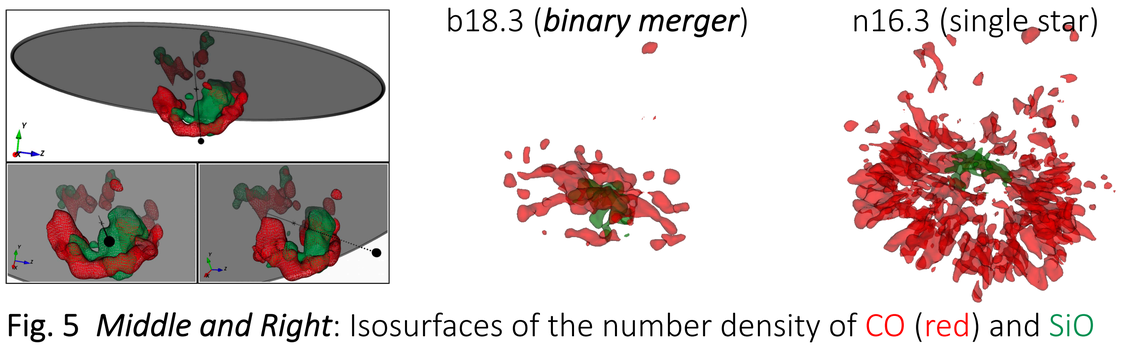

Fig. 5 *Middle and Right*: Isosurfaces of the number density of CO (red) and SiO (green) molecules (30% of the maximum value) at 30 yr after the explosion. By assuming homologuos expansion, the approximate length scale is 10^{17} cm. ***Left***: CO 2−1 (red) and SiO 5−4 (green) emission observed by **ALMA** (Abellán et al. 2017)

Acknowledgement: The numerical computations were carried out complementarily on MARCONI at CINECA, Italy, HOKUSAI at RIKEN, Japan, Cray XC40 at YITP, Kyoto University, Japan and Cray XC30 and XC50 at CfCA, NAOJ, Japan. This research also used computational resources of the K computer provided by the RIKEN Center for Computational Science through the HPCI System Research project (Project ID:hp180281) and the PRACE Research Infrastructure resource Marconi based in Italy at CINECA (PRACE Award N.2016153460).

References: **[1]** Urushibata et al. 2017, MNRAS, 473, L101, **[2]** Ono et al. 2013, ApJ, 773, 161, **[3]** Orlando et al. 2019, A&A, 622, A73, **[4]** Ono et al. 2020, ApJ, 888, 111 **[5]** Orlando et al. 2020 A&A, 636, A22, **[6]** Ono et al. 2020, JPS Conf. Proc., 31, 011029